Directed Transport Born From Chaos

Dima Shepelyansky

Quantware group, Laboratoire de Physique Théorique
CNRS, Université Paul Sabatier, Toulouse, France

http://www.quantware.ups-tlse.fr

Collaboration with

Alexei Chepelianskii (undergraduate, ENS, Paris)

Giampaolo Cristadoro (PhD, Como, Italy => now post-doc at MPI, Dresden)

Discussions: M. Entin and L.Magarill (theory), Kvon Ze Don (experiment)

(Inst. of Semiconductor Physics, Novosibirsk);

J.-C.Portal (experiment, CNRS, Grenoble); H.Linke (U. Oregon);

SUPPORT: ANR PNANO project MICONANO

The Feynman ratchet

Can useful work be extracted out of unbiased microscopic random fluctuations if all acting forces and temperatures gradients average out to zero?
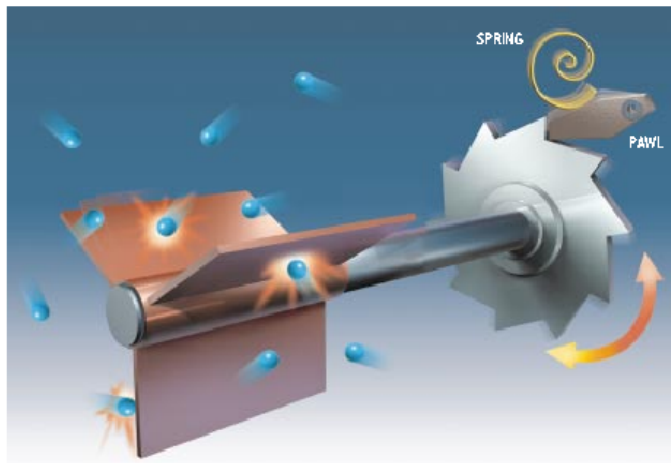
(taken from D.Astumian, Scientific American, July 2001)

Thermal equilibrium: the gas surrounding the paddles and the ratchet (plus the pawl) are at the same temperature

In spite of the built asymmetry no preferential direction of motion is possible. Otherwise, we could implement a perpetuum mobile, in contradiction to the second law of thermo-dynamics

Directed transport born from chaos

A board of rigid disks on a triangular lattice has been invented by Galton in 1889 to demonstrate the appearance of statistical laws from dynamical motion. This system, also called periodic Lorentz gas, has been proved to be completely chaotic by Sinai in 60th. The dynamics remains chaotic also for semidisks scatterers oriented in one direction. Even if the inversion symmetry is broken, the directed transport remains forbidden by the detailed balance principle. This remains true also in presence of polarized monochromatic force produced by microwave radiation. However, when dissipation is present, a new stationary state is born from chaos. It is characterized by a directed transport which can be efficiently controlled by the microwave polarization even if mean force is zero. The transport velocity is proportional to the dissipation rate. Being universal this effect exists also for the Maxwell/Fermi-Dirac thermostatted gas moving between semidisks in presence of a microwave field. Nowadays technology allows to realize the semidisk Galton board with a two-dimensional electron gas in a superlattice of micron size antidots. In this case the theory predicts appearance of strong currents induced by microwave fields. This opens new prospects for high frequency control of transport in presence of dissipation and chaos at nanoscale.

A.D.Chepelianskii and D.L.Shepelyansky

The semidisk Galton board

A particle moves on the semidisk Galton board under the influence of a linearly polarized radiation $\mathbf{f} = f(\cos\theta, \sin\theta)\cos\omega t$, friction force $\mathbf{F}_f = -\gamma\mathbf{v}$ and elastic collisions with semidisks. The disk radius is $r_d = 1$, distance between disk centers $R = 2$, mass $m = 1$.
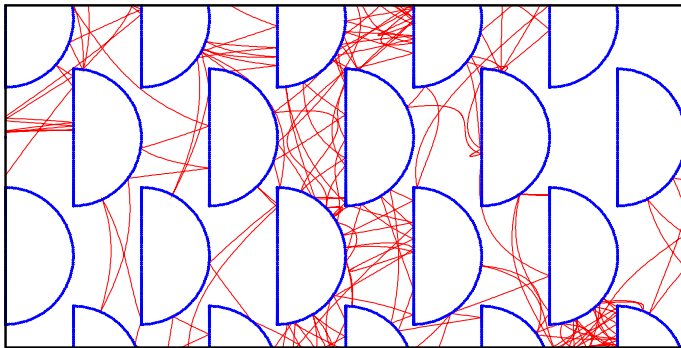

A chaotic trajectory at radiation with $f = 4$, $\theta = \pi/8$, $\omega = 1.5$ and dissipation $\gamma = 0.1$. The trajectory starts near $x = y = 0$, the region shown corresponds to $-27 < x < -17$, $-10 < y < -5$.

NEW material

A.D.Chepelianskii and D.L.Shepelyansky

Polarization dependence
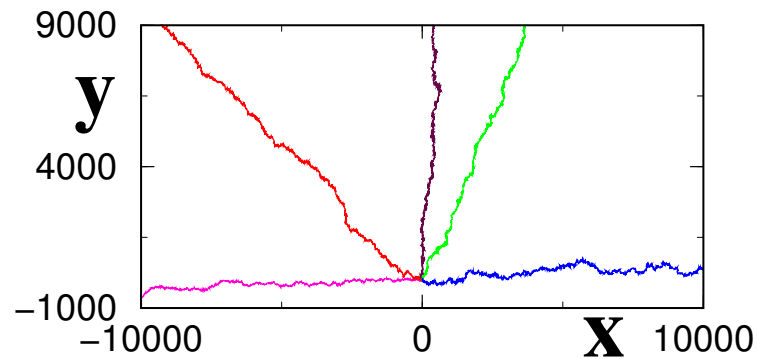
Directed transport for one trajectory at various polarizations of radiation $\theta = 0$, $\pi/8$ (same trajectory as in Fig. 1), 0.21π, $\pi/4$, $\pi/2$ (from left to right clockwise) at $f = 4$, $\omega = 1.5$, $\gamma = 0.1$.
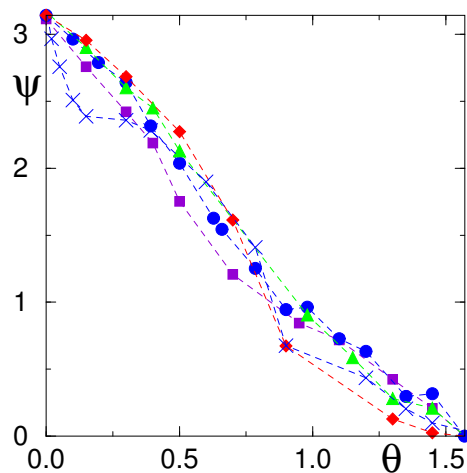

Dependence of flow angle ψ on polarization angle θ, measured in radians, for $f = 4$ and $\omega = 1.5$ at $\gamma = 0.2$ (squares), 0.1 (circles), 0.05 (triangles) and 0.025 (diamonds) and $\omega = 0.1$ at $\gamma = 0.1$ ($\times$). Dashed curves are drown to adapt an eye.

A.D.Chepelianskii and D.L.Shepelyansky

Density distribution
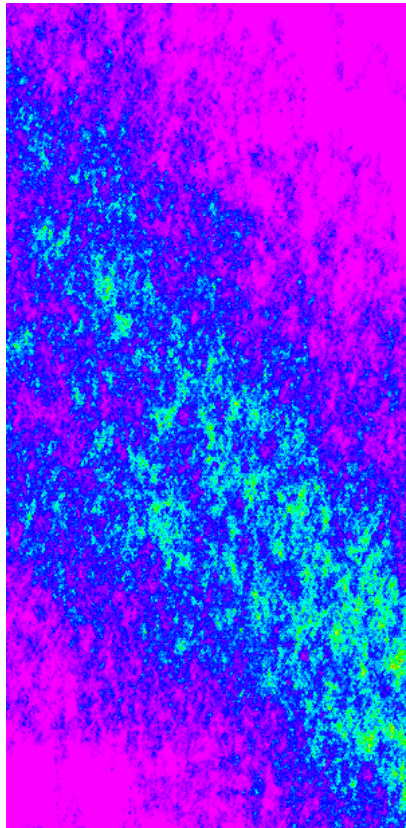
Density distribution in the region $-400 \leq x \leq -100$, $0 \leq y \leq 600$ averaged over 200 trajectories in a time interval $0 \leq t \leq 2 \cdot 10^4$ for parameters of previous Fig.. Initially all trajectories are distributed near $x = y = 0$ with random velocity directions and $v^2 = 1$, density is proportional to color changing from zero (rose) to maximum (green).

Stationary energy
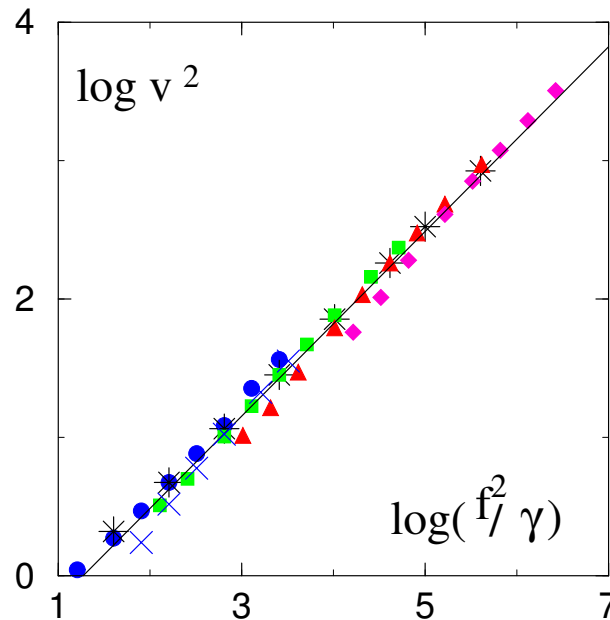
Dependence of average v^2 on f and γ for $\theta = 0$ at $\omega = 1.5$ and $f =$4(circles), 16 (squares), 64 (triangles), 256 (diamonds) and $\gamma = 0.1$ ($*$); the case at $\omega = 0.1$ and $f = 4$ is shown by ($\times$); total interval of parameters variation is $5 \cdot 10^{-3} \leq \gamma \leq 4$, $2 \leq f \leq 256$. The full line gives the dependence $v^2 = (f^2/\gamma)^{2/3}/7$, energy $E = v^2/2$. Logarithms are decimal.

Estimates: the diffusion rate in energy is $D_E = (\Delta E)^2/t \sim \dot{E}^2\tau \sim f^2 vl$ where the mean-free path $l \sim R \sim 1$, the collision time $\tau = l/v \sim R/E^{1/2}$ and the space diffusion rate $D \sim vl$ ($\dot{E} \sim v\dot{v} \sim fv \cos \omega t$). Thus $E = v^2/2 \sim (D_E/\gamma)^{1/2} \sim (lf^2/\gamma)^{2/3} \sim (f^2/\gamma)^{2/3}$
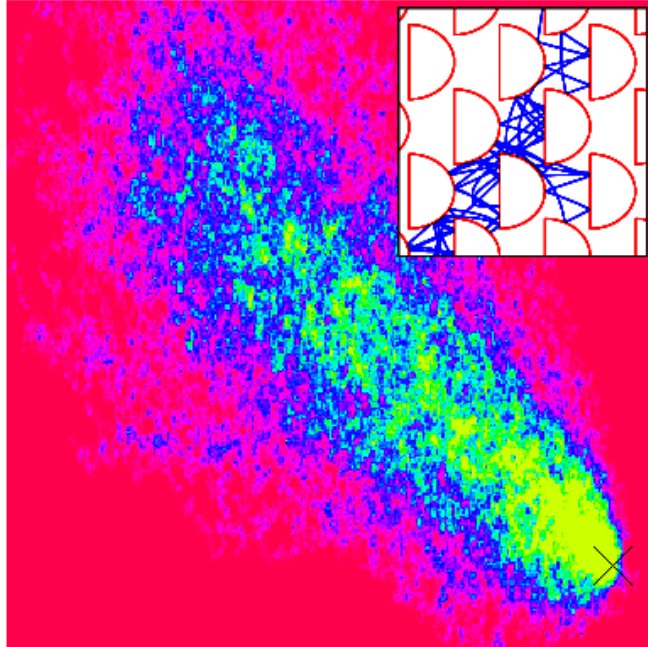
Flow velocity
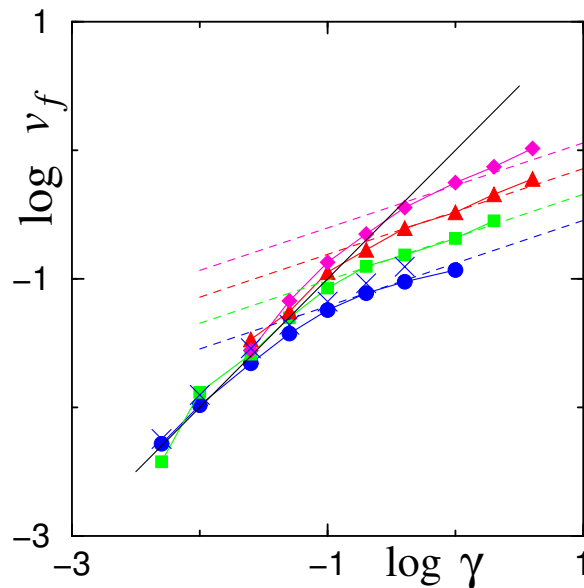
Dependence of the flow velocity v_f on friction γ for $\theta = 0$ and $\omega = 1.5$ at $f = 4$, 16, 64 and 256 and $\omega = 0.1$ at $f = 4$ (same symbols as in previous Fig.). The straight lines show the asymptotic behavior at $\gamma > \gamma_c$ (dashed) and $\gamma < \gamma_c$ (full)

Asymptotic behavior: $v_f \approx l^{2/3}(f\gamma/m^2)^{1/3}/12 \quad (\gamma > \gamma_c)$,
$$v_f \approx l\gamma/m \ (\gamma < \gamma_c),; \ \gamma_c \approx (mf/l)^{1/2}/40$$

# The Nosé - Hoover thermostat dynamics

Density distribution averaged over the time interval $0 \leq t \leq 5 \cdot 10^5$ and obtained from dynamics of 200 particles given by the Nosè-Hoover equations at thermostat temperature $T = 24$. The region of distribution is $x = [-2050, 150]$, $y = [-300, 1900]$. Initially particles are placed at $x = y = 0$ (cross) with random velocities. Density is proportional to color changing from zero (red) to maximum (yellow). The parameters of driving force are $f = 16$, $\omega = 1.5$ and $\theta = \pi/8$. The relaxation time scale of the thermostat is $\tau = \sqrt{50}$. Insert shows one trajectory on small scale moving between semidisks.
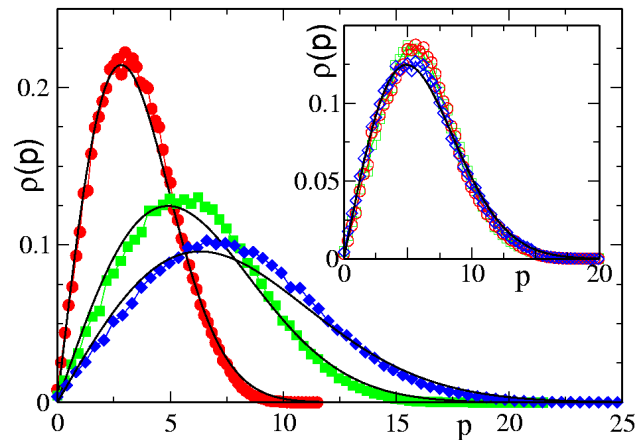
Equations of motion:

$$\dot{\mathbf{q}} = \mathbf{p}/m \quad, \quad \dot{\mathbf{p}} = \mathbf{F} - \gamma\mathbf{p} \; , \quad \dot{\gamma} = [\mathbf{p}^2/(2mT) - 1]/\tau^2$$

The Maxwell distribution
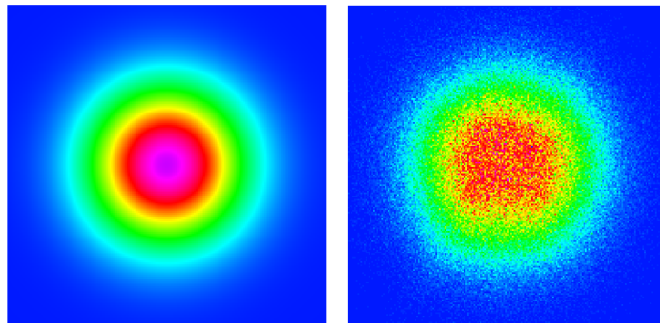
Steady state distribution in 2D momentum plane (p_x, p_y), density is proportional to color changing from zero (blue) to maximum (rose-violet). Left: the Maxwell distribution at temperature of Fig. 1; right: distribution obtained numerically from the Nosè-Hoover thermostat for the case of previous Fig.

Thermal distribution ρ in momentum $p = |\mathbf{p}|$ for different values of temperature $T = 8, 16, 40$, $\tau = \sqrt{50}$. Insert: the stability of thermostat with respect to $\tau^2 = 1$ (circles), 50 (squares), 100 (diamonds) at fixed temperature $T = 24$.

G.Cristadoro and D.L.Shepelyansky

Averaged friction coefficient
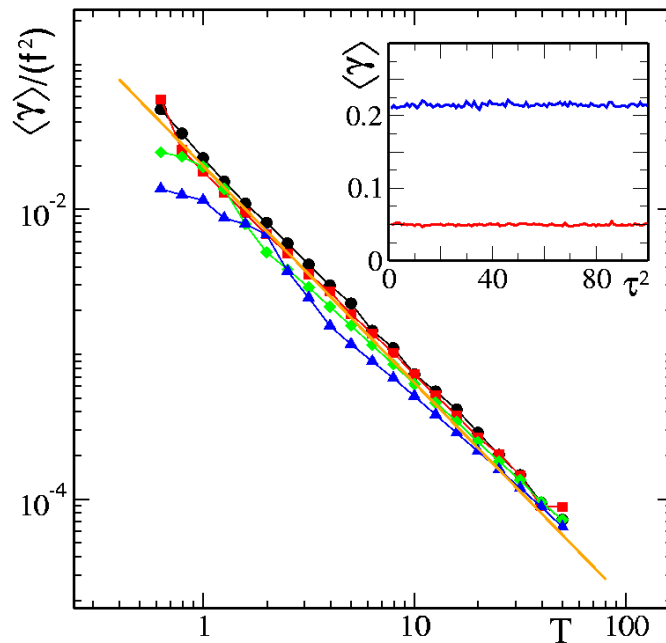
Dependence of rescaled average friction coefficient $\langle\gamma\rangle/f^2$ on temperature T for $f = 4$ (circles), 8 (squares), 16 (diamonds) 32 (triangles) (top to bottom) at fixed $\omega = 1.5$, $\theta = 0$, $\tau^2 = 50$. The straight line shows theory dependence with $C = 0.02$. Insert shows that $\langle\gamma\rangle$ is robust against variation of τ^2 in the interval $[1,100]$ (with step 1); data are shown for $f = 16$, $\omega = 1.5$, $\theta = 0$, $T = 8$ (top curve) and 24 (bottom curve).

Dependence: $\langle\gamma\rangle = C r_d m^{-1/2} f^2/T^{3/2}$, $C \approx 0.02$

$$E^2 \sim D_E/\gamma \sim T^2, \quad D_E \sim f^2 R\sqrt{(T/m)}; \quad E \sim T.$$

G.Cristadoro and D.L.Shepelyansky

Flow velocity in presence of thermostat
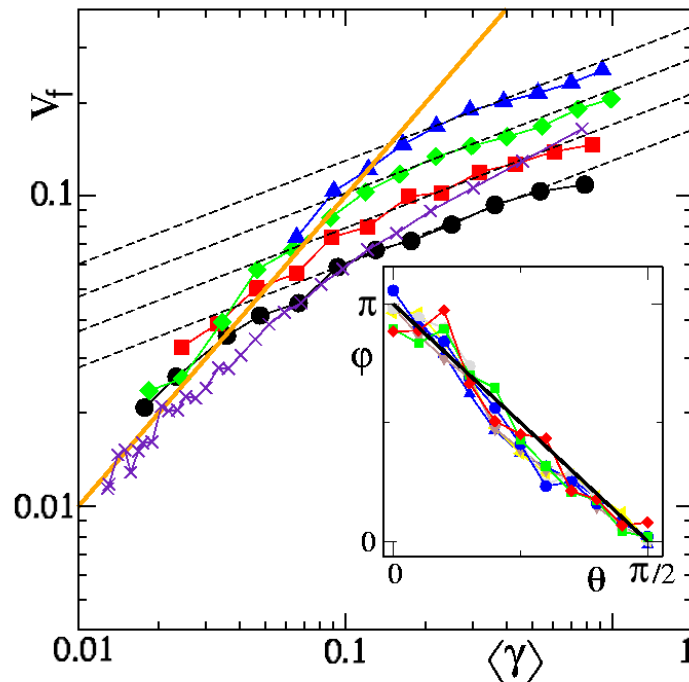
Dependence of the absolute value of average velocity of particle flow v_f on average friction $\langle \gamma \rangle$ for the parameters of Fig. 4 with $f = 4, 8, 16, 32$ (same symbols, from bottom to top). Dashed lines show the scaling dependence $v_f \sim (f\langle\gamma\rangle)^{1/3}$ at large $\langle\gamma\rangle$ for different f values; the full line shows scaling $v_f = \langle\gamma\rangle$ at small $\langle\gamma\rangle$. Crosses show data for the same parameters as for squares ($f = 8$) but with additional circular scatterer added in the center of unit cell to eliminate orbits with a straight flight through the whole system (see text). Insert shows the dependence of flow direction angle φ on polarization angle θ; data are given for $f = 8$, $\omega = 1.5$, $\tau^2 = 50$ and $4 \leq T \leq 11$; full line shows average dependence $\varphi = \pi - 2\theta$.

Dependence: $v_f/v \approx r_d f/50T$, $(T < T_c)$;
$v_f/v \approx (r_d f/8T)^2$, $(T > T_c)$; $v = (2T/m)^{1/2}$, $T_c \approx r_d f$

G.Cristadoro and D.L.Shepelyansky

The Fermi-Dirac thermostat (estimates)

Here the particle velocity v is equal to the Fermi velocity $V_F = (2E_F/m)^{1/2}$ independent of T. This modification gives the average friction γ_F for the Fermi gas

$$\gamma_F = Cf^2 V_F r_d/T^2 \approx v_f/r_d , \qquad (1)$$

where we kept the same numerical constant $C \sim 1/50$. In fact this follows from $D_E \sim f^2 V_F r_d$ and $\gamma_F \sim D_E/T^2$. The second equality appears due to the fact that $E_F \gg T_c$ implying the regime with $v_f \sim \gamma_F r_d$. A small fraction T/E_F of electrons near E_F contributes to this ratchet flow (Pauli blockade ??). Hence, the current I per one semidisk row is

$$I \sim e r_d n_e v_f T/E_F \sim C e r_d^3 \sqrt{n_e} f^2/(T\hbar) . \qquad (2)$$

where we used that for the 2D electron Fermi gas $E_F = \pi n_e \hbar^2/m$. In semiconductor antidot lattices the effective mass m is about 15 times smaller compared to the electron mass.

# The Fermi-Dirac thermostat with the Metropolis algorithm I
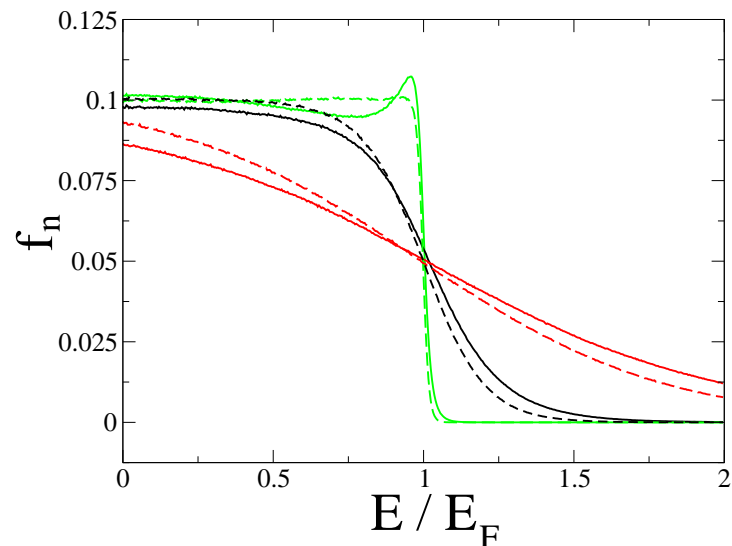
Energy distribution for $T/E_F =).01, 0.10.4$ (green, black, red curves); for dashed curves $f = 0$, for full curves $fr_d/E_F = 0.5; E_F = 10, \omega = 1, R/r_d = 2$. Dashed curves coinsides with the corresponding Fermi-Dirac distribution.

An effective solution of the Vlasov-Ühling-Uhlenbeck equation:

$$\frac{\partial f_V}{\partial t} + \mathbf{v}\frac{\partial f_V}{\partial \mathbf{r}} + \mathbf{F}(\mathbf{r}, t)\frac{\partial f_V}{\partial \mathbf{p}} = I_{cc} = -(f_V - f_0)/\tau_{rel}$$
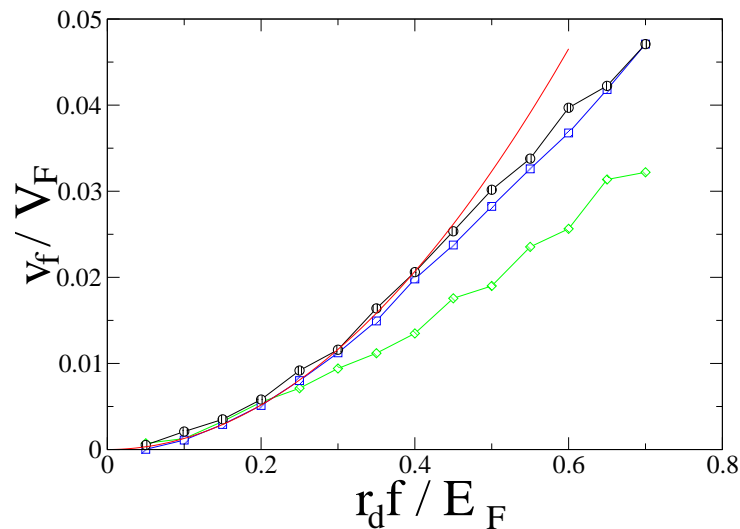
The Fermi-Dirac thermostat with the Metropolis algorithm II
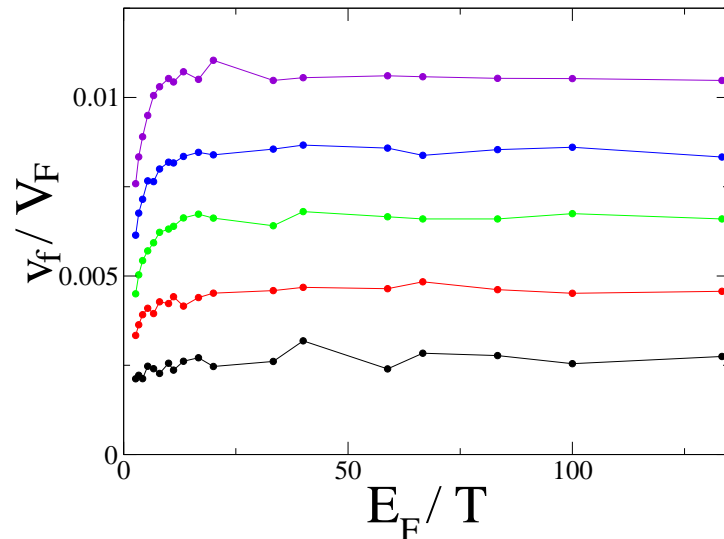
Dependence of the rescaled flow velocity v_f/V_F on the rescaled inverse temperature E_F/T, different curves correspond to $f = 7, 6, 5, 4, 3$ (from top to bottom). Here $\omega = 1$, $R = 2$, $r_d = 1$, $\theta = 0$, $E_F = 10$.

NO Dependence on Temperature T !
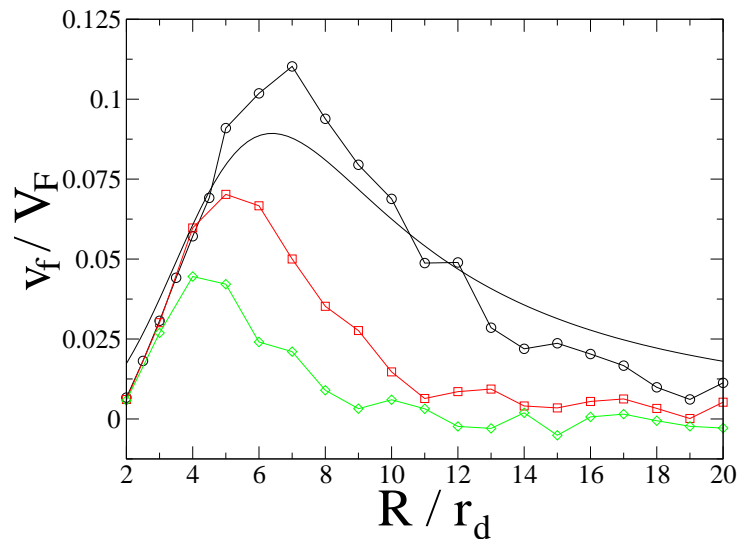(same result by M.Entin, L.Magarill, PRB **73**, 205206 (2008))

Dependence on microwave power

The rescaled flow velocity v_f/V_F as a function of rescaled applied force fr_d/E_F for different $T/E_F =$ 0.4 (green), 0.1 (blue), 0.01 (black); quadratic field dependence is shown by red; here $\omega = 1$, $R = 2$, $r_d = 1$, $\theta = 0$, $E_F = 10$.
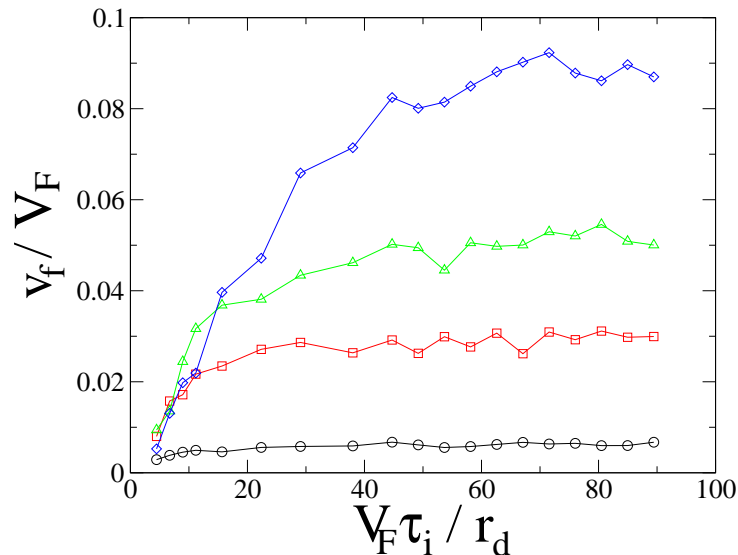
Dependence: $v_f/V_F = C(r_d f/E_F)^2; C \approx 0.13$

Dependence on lattice constant R

The rescaled flow velocity v_f/V_F as a function of rescaled lattice constant R/r_d for different $\omega = 1$ (black), 1.5 (red), 2.0 (green); here $T/E_F = 0.1, f = 5$, $r_d = 1$, $\theta = 0$, $E_F = 10$.

Dependence:
$$v_f/V_F = \frac{R^2 f^2}{E_F^2} \frac{A}{1 + B(\omega R^2/r_d V_F)^2};$$
$$A \approx 0.017, B \approx 0.012$$

Effects of scattering on impurities

Dependence of v_f/V_F on rescaled scattering time $\tau_i V_F/r_d$ for different $R/r_d = 6, 4, 3, 2$ (from top to bottom); at $T/E_F = 0.1$, $f = 5$, $r_d = 1$, $\theta = 0$, $E_F = 10$. Optimal choice: $R \sim V_F\tau_i$. Effect disappears if the Larmor radius is smaller than R (data not shown).

Current per row: $I = \sqrt{3}en_eRv_f \approx emf^2R^3/(50n_e^{1/2}\hbar^3)$

Experimental conditions

For the 2D electron Fermi gas $E_F = \pi n_e \hbar^2/m = mV_F^2/2$. In semiconductor antidot lattices the effective mass m is about 15 times smaller compared to the electron mass. For a typical parameters of semidisk antidot lattice with electron density $n_e \sim 10^{12} cm^{-2}$, $R \sim r_d \sim 1\mu m$, field strength per electron charge $f/e \sim 1V/cm$ we obtain $v_f/V_F \sim 10^{-4}$. At these parameters $E_F \sim 150K$, $V_F \sim 3 \cdot 10^7 cm/sec$ and the current is $I \sim 0.1nA$ (usual $T \sim 10K$). For $R \sim 5\mu m > r_d \sim 1\mu m$ this gives a strong current per row of $10nA$.

At $R \sim r_d \sim 1\mu m$ the ratchet effect should disappear at a magnetic field $B \sim 0.1T$ when the Larmor radius becomes smaller than R.

Quantum effects: The above result is based on the semiclassical estimate for the diffusion rate D_E which assumes that the energy of microwave photon is larger than the level spacing Δ inside one unit cell: $\hbar\omega > \Delta \approx 2\pi\hbar^2/(mr_d^2)$. In the opposite limit $\hbar\omega \ll \Delta$, ac-driving is in the quantum adiabatic regime.

In experiments of H.Linke *et al.*, Science **286**, 2314 (1999) the frequency was in a deep adiabatic regime with very low $\omega/2\pi \sim 100Hz$ (overdamped case) and nonlinear regime played an important role.
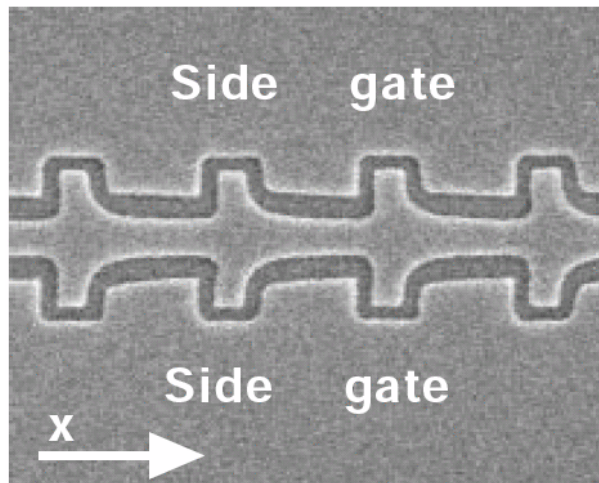
Experiments in Grenoble: on the way
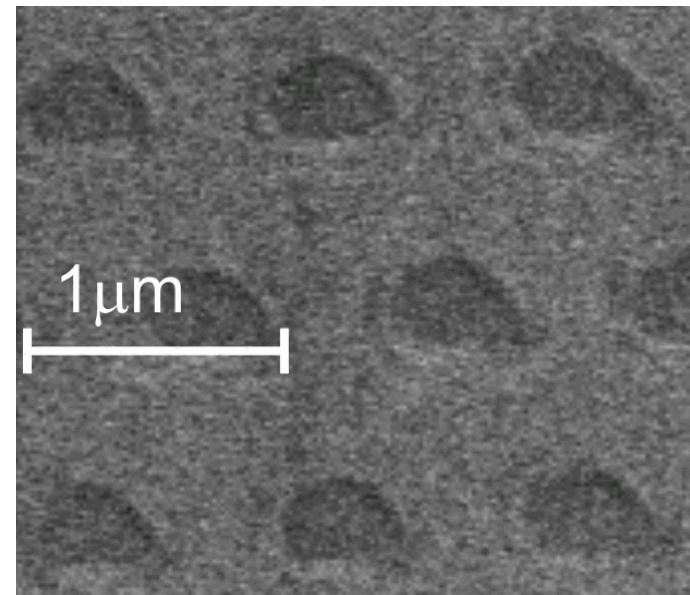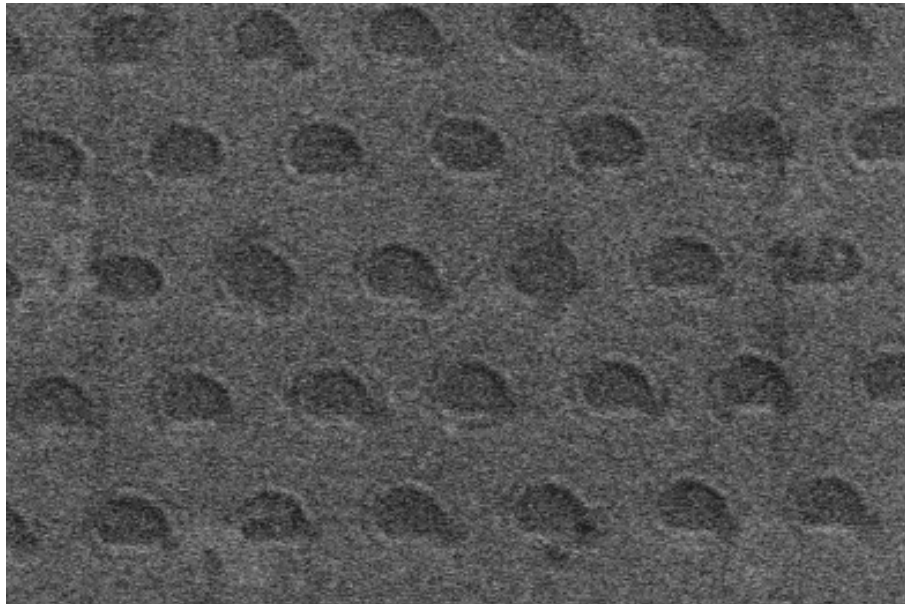
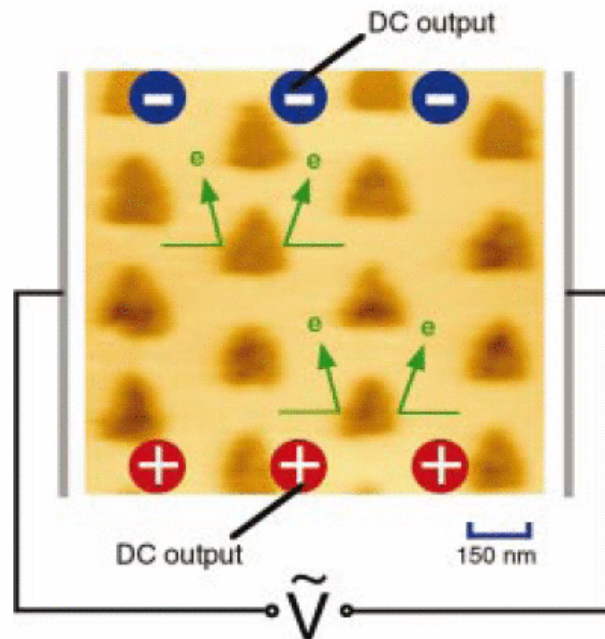# Room-temperature experiments with InGaAs/InP in 2001

FIG. 1. (Color) An atomic force microscope image of the nanomaterial is shown. Each etched triangular hole (obstacle) scatters electrons in a predetermined upward direction independent of the direction of the applied field, as illustrated by the arrows. Therefore, dc signals are generated even when ac or random fields are applied.
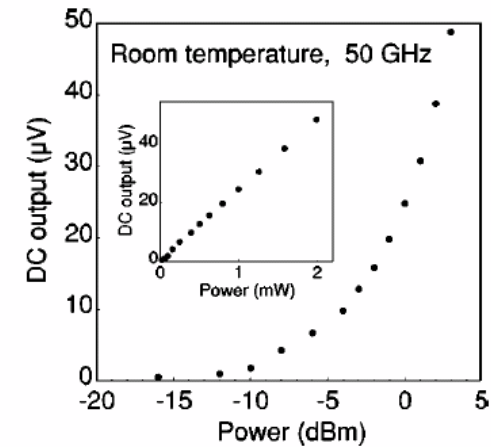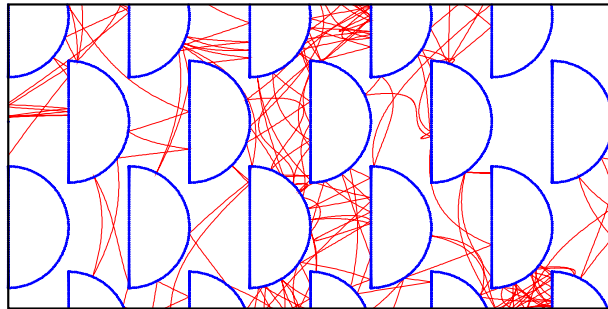

FIG. 3. dc output of a piece of the nanomaterial as a function of the power of the 50 GHz signal, which is applied to the material via coplanar probes is shown. The power units are dBm in the main curve and mW in the inset.

Also A.Lorke, S.Wimmer, B.Jager et al. Physica B **249**, 251 (1998)

Conclusions:

New NANO-GORE-TEX material

Room-temperature Applications: sensors, detectors ...